Fuel 277 (2020) 117932

Contents lists available at ScienceDirect

Fuel

journal homepage: www.elsevier.com/locate/fuel

Full Length Article

High-pressure direct injection of methanol and pilot diesel: A non-premixed dual-fuel engine concept

Yabin Dong[a], Ossi Kaario[a,*], Ghulam Hassan[a], Olli Ranta[a], Martti Larmi[a], Bengt Johansson[b]

[a] Aalto University, School of Engineering, Department of Mechanical Engineering, Finland
[b] King Abdullah University of Science and Technology, Clean Combustion Research Center, Saudi Arabia

ARTICLE INFO

Keywords:
Methanol
Direct-injection
Dual-fuel
Non-premixed combustion
Two-injector cylinder head configuration
Emission reduction

ABSTRACT

In order to reduce the climate impacts, methanol produced from carbon-neutral methods plays an important role. Due to its oxygen content and high latent heat, methanol combustion can achieve low soot and NO_x emissions. In the present study, direct injection (DI) of methanol is investigated in a non-premixed dual-fuel (DF) setup with diesel pilot. The present DF engine study is carried out via a specially-designed new cylinder head operating with a centrally located methanol injector and with an off-centered diesel pilot injector. The target is to inject methanol close to top dead center (TDC) in a similar fashion as in standard diesel combustion enabling robust operation with high efficiency. The ignition of the DI methanol is achieved with an almost simultaneously injected diesel pilot. The experiments were conducted in a single-cylinder heavy-duty research engine at a constant engine speed of 1500 rpm with a compression ratio of 16.5. The indicated mean effective pressure (IMEP) varied between 4.2 and 13.8 bar while the methanol substitution ratio was swept between 45 and 95%. In addition, the diesel pilot and methanol injection timings were varied for optimum efficiency and emissions. The introduced non-premixed DF concept using methanol as the main fuel showed robust ignition characteristics, stable combustion, and low CO and HC emissions. The results indicate that increasing both the load and the methanol substitution ratio can increase the thermal efficiency and the stability of combustion (lower COV) together with decreased CO and HC emissions.

1. Introduction

Oil products accounted for more than 90% of the transportation sector fuel consumption in 2016 [1] while internal combustion engines were the dominating power source in this sector. Diesel engines are superior in the heavy-load agriculture and marine sector owing to their high fuel conversion efficiency, power capability, and operating range [2]. However, diesel engines have problems related to NO_x, particulate matter, and to some extent greenhouse gas (GHG) emissions. With increasing concerns on climate change, advanced engine technologies and alternative fuels are needed to mitigate the use of fossil fuels and reduce carbon emissions [3,4]. Widely studied advanced engine technologies include dual-fuel (DF) engines [5], homogeneous charge compression ignition engines (HCCI) [6], premixed charge compression ignition engines (PCCI) [7], and reactivity controlled compression ignition engines (RCCI) [8]. This paper will primarily focus on an improved DF engine concept.

DF engine technology, where the main fuel energy comes from a low-reactivity fuel (i.e. methane, natural gas, biogas, CNG, ethanol, and methanol) and the ignition energy is provided by a high-reactivity fuel (i.e. diesel and n-heptane) [9,10,11,12], is a well-known technology for robust engine operation with decreased environmental impact [13,14,15]. Traditionally, the approach to deliver the low-reactivity fuel is via the intake manifold (port fuel injection, PFI) to create a homogeneous fuel-air mixture. Owing to the small quantity of pilot diesel, the lean premixed combustion of the main fuel yields low NO_x and soot emissions [16,17,18]. Applying methanol as the low-reactivity fuel can further reduce NO_x and soot emissions due to its oxygen content and high latent heat of evaporation [19,20,21]. Traditionally, methanol is produced from the syngas (mixture of CO, CO_2, and H_2) synthesis reaction, where the syngas is mainly produced from coal and natural gas [22]. With increasing concern for the environment, a variety of low-carbon methanol synthesis technologies have been developed. For example, the Power-to-Liquid (PtL) approach can be applied to synthesize methanol directly, where renewable based H_2 (i.e. water electrolysis by renewable electricity or biomass gasification and reforming) and recovered CO_2 from industrial processes can be used for methanol synthesis [23,24].

* Corresponding author.
E-mail address: ossi.kaario@aalto.fi (O. Kaario).

https://doi.org/10.1016/j.fuel.2020.117932
Received 12 February 2020; Received in revised form 4 April 2020; Accepted 23 April 2020
Available online 05 June 2020

Nomenclature

ATDC	After top dead center
°CA	Crank angle degree
CA5	Crank angle of 5% cumulative heat
CA50	Crank angle of 50% cumulative heat
CA90	Crank angle of 90% cumulative heat
CI	Compression ignition
COV	Coefficient of variation
DDur	Diesel injection duration
DI	Direct injection
DSOI	Diesel start of injection
FPGA	Field-programmable gate array
$FuelMEP_{Diesel}$	Diesel mean effective pressure
$FuelMEP_{Methanol}$	Methanol mean effective pressure
HC	Unburned hydrocarbon
HPDI	High-pressure direct injection
HRR	Heat release rate
IMEP	Indicated mean effective pressure
ITE	Indicated thermal efficiency
LHV	Lower heating value
MDur	Methanol injection duration
MSOI	Methanol start of injection
MSR	Methanol substitution ratio
PFI	Port fuel injection
∅	Equivalence ratio
λ	Lambda 1/∅

Despite many desirable properties of methanol, its low cetane number brings ignition problems. In PFI methanol engine, increasing the compression ratio and raising the intake air temperature is a common approach to improve the ignition characteristics [25,26,27]. A PFI methanol engine study conducted by Pan et al. [25] shows that increasing the charge air temperature can reduce ignition delay and diminish the HC and CO emissions. The proportion of the methanol energy content is a critical parameter in DF engines, and it is normally below 50% due to unburned methanol emissions at a high methanol substitution ratio [20,25]. Moreover, Li et al. [19,21] found that high pilot injection pressure enhances fuel atomization and decreases cycle-to-cycle variation. Additionally, advancing pilot injection can reduce ignition delay, increase brake thermal efficiency and reduce HC emissions, but it may lead to high NO_x emissions and rapid combustion before TDC [20,28]. Overall, the operation of PFI DF engines requires a careful optimization of several parameters such as fuel injection strategy [29,30], air intake temperature, energy fraction from low-reactivity fuel [31,32], compression ratio, equivalence ratio [33,34], and exhaust gas recirculation [35].

Contrary to the PFI concept, the present study utilizes a two-injector high-pressure direct injection (DI) system to deliver both diesel and methanol. Unlike methanol PFI configuration where methanol is injected to the intake manifold, here methanol is directly injected into the combustion chamber. Ignition is provided by a short high-pressure diesel pilot. The ignited diesel will act as an efficient spark for the high-pressure methanol sprays yielding a non-premixed combustion. According to the literature, such a system is rarely studied with limited references [36,37]. In particular, the control strategy on the engine platform is less investigated and the HC emissions of the non-premixed methanol high-pressure DI are unknown. A published study conducted by Jia et al. [37] tested the high-pressure DI of methanol and compared it with PFI methanol configuration. However, the study of Jia aimed to achieve RCCI combustion (premixed methanol as the main fuel). The experiments conducted by Jia et al. [37] are principally distinctive to the present study because the present research does not aim to achieve homogeneous fuel air mixture but rather aiming at investigating the non-premixed methanol combustion.

With similar setup to the present paper, a methanol high-pressure DI configuration is studied by Wang et al. [36] on a constant volume combustion chamber, which provides certain theoretical guidance on the interaction between methanol and diesel. The experimental study aimed to understand the diesel and methanol interaction during the combustion process. It was found that the flame spread faster towards the path of diesel injection but slower towards the path of methanol. Moreover, the research of such configuration of natural gas provides practical references for the operation of the present study. Faghani et al. [38,39] conducted research on a natural gas high-pressure direct injection (HPDI) with a diesel pilot DF engine. To achieve DI of both natural gas and diesel pilot, a specially-designed injector by the Westport Fuel System was applied. The injector was able to deliver both fuels independently through different holes. With a 17:1 compression ratio, the engine was successfully operated with natural gas energy

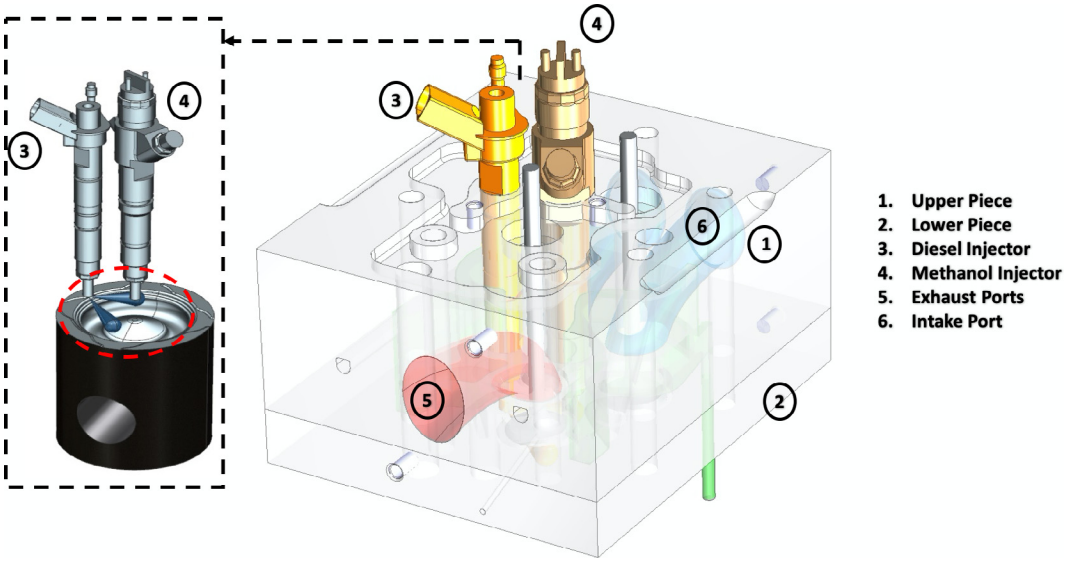

Fig. 1. Two-injector, Three-valve Cylinder Head Design.

content between 90 and 95%. It was also found that particulate matter and methane emissions were reduced by a split gas injection strategy. Hence, the high-pressure DI methanol injection configuration of the present study has the potential to achieve 1) high efficiency with diesel-like combustion process and 2) low emissions as methanol has oxygen in the molecule and very high latent heat. The robust diesel pilot combustion which triggers the methanol ignition has advantages such as flexible operation owing to the direct injection of methanol and diesel pilot. It is expected that the charge temperature and ignition controllability have significantly reduced sensitivity compared to PFI methanol strategy.

To better understand the non-premixed methanol-diesel configuration, the current study presents an experimental investigation of DI high-pressure methanol injection with a diesel pilot on a single cylinder DF engine. We designed a special cylinder head (Section 2.1) to accommodate both methanol and diesel injectors. The pilot diesel fuel is injected ahead of methanol to create high-temperature and high-pressure environment for robust methanol ignition. The methanol quantity is increased to investigate the high methanol substitution ratio operation and fuel injection timing is varied to improve the DF engine operation. The combustion characteristics, combustion stability, indicated thermal efficiency, and emissions are studied in this experiment.

2. Experimental setup and methods

2.1. Cylinder head

In order to ignite the direct-injected methanol sprays by a diesel pilot, a specially-designed cylinder head with two injectors and three valves was designed for the present study. Fig. 1 illustrates a 3D model of the cylinder head, as well as the injector-piston position in the combustion chamber. Both diesel and methanol injectors can be installed on the new cylinder head. A two-hole Bosch piezo injector delivers pilot diesel, and the fuel direction is towards the center of the combustion chamber as shown in Fig. 1. Both fuels are injected at the end of compression stroke preparing for the diffusion combustion. The diesel pilot injection starts at a few crank angle degrees earlier than the methanol injection, so that the burning diesel can create a high-temperature and high-pressure environment for the methanol sprays. The diesel pilot injection is starting at few crank angles earlier than the methanol injection, so that the burning diesel can create a high-temperature and high-pressure environment for the methanol sprays. The cylinder head is divided into upper and lower pieces for manufacturing purposes. Three-valve configuration (two intake ports, a single exhaust port) is designed to create room for the diesel pilot injector. The inlet contains two-direct zero-swirl intakes ports, while a single exhaust port has the same profile as the original factory cylinder head. An extruded buffer joint is created between the upper and lower piece to release thermal stress. According to a CFD analysis, during the engine running time, the highest temperature may occur at the bottom deck close to injector tips due to manufacturing constraints.

2.2. Test engine setup

The test engine is a single-cylinder research engine modified from a commercial AGCO 84 AWI 6-cylinder common rail in-line heavy-duty engine. Table 1 lists the technical specifications of the research engine and Fig. 2 shows the test engine layout. The engine is equipped with an AC electric motor either to brake the crankshaft or to maintain the required engine speed. An externally powered industrial air compressor (GARDNER DENVER VS 25) simulates the function of a turbocharger. An electronic valve and a butterfly valve are installed to control intake charge pressure and exhaust backpressure respectively. Both the intake and exhaust side are equipped with pulse reservoirs to absorb pressure vibrations. The research engine valve is controlled by an electro-hydraulic valve actuator system, EHVA (DYNASET), by which users can freely define the valve-lifting curve. Diesel and methanol have separate delivery systems both supplied with a high-pressure pump. Diesel is delivered by a two-hole piezo injector (Bosch CRI3-20), and an eight-hole solenoid injector is used for methanol (Bosch CRIN2-16). Users control all physical parameters through a customized LabView software on local PC which communicates with a field-programmable gate array (FPGA) from National Instruments and a real-time computer. A piezo pressure sensor (KISTLER 6045AU20) is installed in the combustion chamber to detect cylinder pressure. The pressure signal passes through a pressure amplifier (KISTLER 4665) and is recorded by the real-time computer. Type-K thermal couples are used to measure the temperature of the engine, charge air, exhaust, engine water, and exhaust valve seat. Charge air mass flow and fuel rail pressure are regulated by PID-controllers. Emission samples pass through a continuous emission monitoring system where the sample line is constant at 191 °C to measure NO_x, HC, CO, CO_2, and O_2 emissions. NO_x is measured by an ECO physics analyzer via chemiluminescence, a flame ionization detector provided by J.U.M. Engineering is used to detect HC emissions and a SICK Sidor nondispersive infrared sensor analyzes CO/ CO_2/ O_2 emission.

2.3. Diesel and methanol fuel

The diesel used in the experiments complies with the European EN590 diesel standard. The main fuel is commercial methanol with 99.9% purity. In this study, 1% ETHOMEEN O/12 of methanol weight is added in the methanol tank for the lubrication. Table 2 lists the general properties of diesel and methanol. It is noted that methanol has much lower energy content and cetane number compared to diesel. However, the auto-ignition temperature of methanol is much higher and the heat of vaporization is four times higher than that of diesel.

2.4. Test method and conditions

The experiment is conducted at a constant engine speed of 1500 rpm. The rail pressure of the diesel pilot is set up at 1200 bar and the methanol rail pressure is constant at 1000 bar. Sufficient airflow sustains the diffusion combustion and the global λ is above 1.7 in the whole experiment. To investigate the maximum methanol substitution ratio (MSR) in this DF configuration, the methanol quantity test was first carried on via increasing methanol injection duration (MDur). In addition, the start of injection (SOI) was varied for both fuels to assess the effect on combustion and emission characteristics. All test points are run for five minutes for stabilization.

The combustion stage of the present methanol high-pressure DI is analyzed via the 2nd derivative of the heat release curve. It is a novel method recently applied by Ahmad et al. [40]. This method identifies the local maxima of the 2nd derivative of HRR as the transition points

Table 1
Research Engine Specifications.

Engine Type	Single-cylinder, direct injection*
Bore × stroke [mm]	111 × 145
Displacement [L]	1.4
Compression ratio	16.5
Fuel injection system	Common rail high pressure direct injection
Intake valve open	356° ATDC
Intake valve close	−155° ATDC
Exhaust valve open	150° ATDC
Exhaust valve close	380° ATDC
Diesel injector	Bosch CRI3-20, two-hole piezo injector, Nozzle hole diameter. 0.110 mm
Methanol Injector	Bosch CRIN2-16, eight-hole solenoid injector, Nozzle hole diameter. 0.218 mm

*The single-cylinder research engine is modified from a common rail, in-line, heavy-duty commercial 6-cylinder engine.

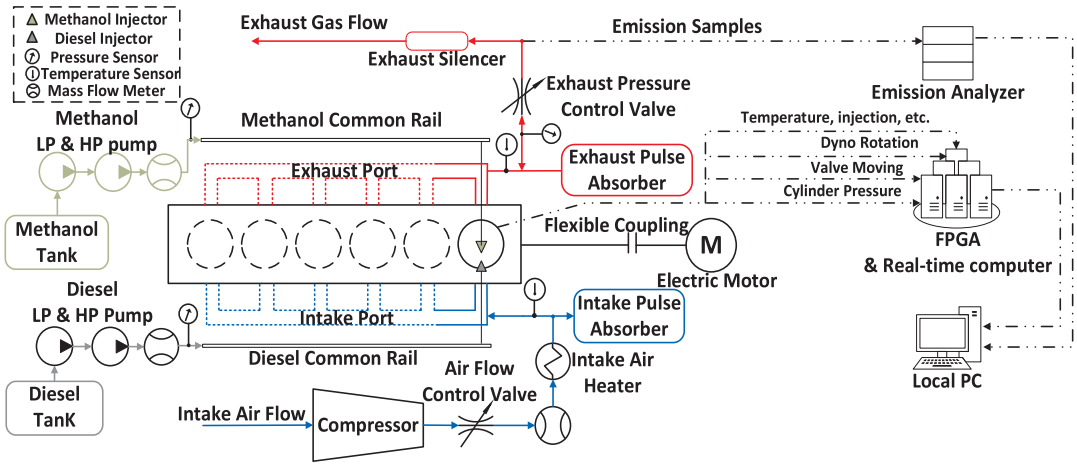

Fig. 2. Research Engine Layout.

Table 2
Diesel and methanol fuel properties [20,21].

Property	Diesel	Methanol
Cetane number	≥51	3–5
Auto-ignition temperature [°C]	250	450
LHV [MJ/kg]	43	20.3
Heat of vaporization [kJ/kg]	250	1150
Density at 20 °C [kg/m^3]	830	790
Viscosity at 20 °C [mPa.s]	2.8	0.59
Stoichiometric air fuel ratio	14.7	6.45
Content of C [%]	86	37.5
Content of H [%]	14	12.5
Content of O [%]	0	50

* Methanol contain 1 wt% of ETHOMEEN O/12 lubricant.

of combustion [40]. The following equation illustrates the identification of transition points θ_i, where $\theta_{minima,I}$ represents the $i \in (int; i > 0)$ minima point on the 2nd derivative curve of HRR, and $\theta minima_{,\,i+1}\theta i$ is the $i + 1$ minima point. The start of combustion is defined based on five percent of the cumulative heat release rate (CA5) while the end of combustion is defined based on ninety percent of the cumulative heat release rate (CA90).

$$\theta_i = \theta \Big|_{\max \frac{d^2(HRR)}{d\theta^2}, \{\theta \mid \theta_{minima,i} < \theta < \theta_{minima,i+1}\}} \quad (1)$$

To represent the results in general cases, fuel quantity (controlled by fuel injection duration) is characterized by the measure of fuel mean effective pressure (FuelMEP) [41] that links fuel energy content and IMEP. It is calculated by the following equations, where $\dot{m}_{fuel}$ represents either diesel or methanol, and V_{disp} is the displacement volume of the engine cylinder. Diesel mean effective pressure ($FuelMEP_{Diesel}$) and methanol mean effective pressure ($FuelMEP_{Methanol}$) are calculated separately. The total FuelMEP is the sum of both $FuelMEP_{Methanol}$ and $FuelMEP_{Diesel}$.

$$FuelMEP = \sum_{AllFuels} \frac{\dot{m}_{fuel} \times LHV_{fuel}}{V_{disp}} \quad (2)$$

In the methanol quantity study, IMEP is increased from 4.17 bar to 13.78 bar, and MSR incremented from 45.3% to 95.3%. In order to examine a wide range of MSR, the diesel pilot injection duration is also adjusted. When diesel injection duration (DDur) is constant at 0.95 ms, methanol injection duration is first increased from 0.65 ms to 1.15 ms. Then, diesel injection duration is decreased to 0.2 ms, while the methanol injection duration is increased from 1 ms to 2 ms to reach high MSR. As a result, a higher quantity of methanol mass flow led to the rise of IMEP and MSR. The test group attempts to compare the combustion and emission characteristics through the operation from low-IMEP – low MSR to high-IMEP – high-MSR. In the present study, MSR is calculated from:

$$MSR = \frac{\dot{m}_{methanol} \times LHV_{methanol}}{\dot{m}_{diesel} \times LHV_{diesel} + \dot{m}_{methanol} \times LHV_{methanol}} \times 100\% \quad (3)$$

where $\dot{m}_{methanol}$ and $\dot{m}_{diesel}$ are methanol and diesel mass flow; $LHV_{methanol}$ and LHV_{diesel} are the energy contents of methanol and diesel fuel, respectively.

In the fuel SOI test, DSOI/MSOI with a constant two-degree injection gap was advanced from −9/−7 °CA ATDC to −13/−11 °CA ATDC, which aims to investigate the effects of combustion phase on DF combustion and emission performances. Afterward, only pilot DSOI was advanced from −12 °CA ATDC to −16 °CA ATDC, which aims to

Table 3
Experimental test matrix.

	Operation conditions			
	Methanol Quantity Increasing I	Methanol Quantity Increasing II	DSOI/MSOI Advancing	DSOI Advancing
Engine speed [rpm]	1500	1500	1500	1500
Net IMEP [bar]	4.17–9.18	4.39–13.78	6.23	6.23
DSOI [°ATDC]	−10	−12	−9 to −13	−12 to −16
MSOI [°ATDC]	−6	−10	−7 to −11	−10
$FuelMEP_{Diesel}$ [bar]	6.61	1.49	1.49	1.49
$FuelMEP_{Methanol}$ [bar]	5.46–16.07	10.66–30.44	12.11	12.11
Diesel Mass flow [g/cyc]	0.0216	0.0049	0.0055	0.0051
Methanol Mass flow [g/cyc]	0.038–0.111	0.074–0.210	0.085	0.083
MSR [%]	45.3% to 70.8%	87.6% to 95.3%	88%	88%
Air intake temperature [°C]	24.8	22.4	18.1	18.9

*Methanol injection pressure is 1000 bar and diesel injection pressure is 1200 bar for all test points.

investigate the effects of combustion phasing and emissions. Afterwards, only pilot DSOI was advanced from −12 °CA ATDC to −16 °CA ATDC, which aims to investigate the optimal pilot injection timing. The IMEP was constant at 6.23 bar. CA5, CA50, and combustion duration are identified from the HRR curve. Besides, the coefficient of IMEP variation (COV_{IEMP}) is calculated by Eq. (4) to assess the combustion stability when increasing the methanol quantity and advancing the fuel SOI.

$$COV_{IMEP} = \frac{\delta_{IMEP}}{\overline{IMEP}} \times 100\% \quad (4)$$

where δ_{IMEP} represents the standard deviation of IMEP and $\overline{IMEP}$ stands for the average of IMEP of 100 recorded working cycles.

3. Results

3.1. Effects of methanol quantity

3.1.1. Combustion characteristics

Previous DF engine studies mostly concentrate on port fuel injection of the main fuel and recognize three stages of combustion: diesel pilot diffusion flame, premixed main fuel ignition, and premixed flame propagation [33,40,42,43]. In contrast to premixed combustion, the present study follows the conceptual diesel model developed by John E. Dec [44] and analyzes the non-premixed combustion stages of high-pressure direct methanol injection with a diesel pilot.

Test conditions are listed in Table 3. The trends of MSR and IMEP when increasing methanol quantity are visualized in Fig. 3. First, the diesel mean effective pressure ($FuelMEP_{Diesel}$) was constant at 6.61 bar and MSR was increased from 45.3% to 70.8%. Then, $FuelMEP_{Diesel}$ was reduced to 1.49 bar to further increase MSR. As a result, the experiment succeeded in operating the MSR between 87.6% and 95.3%. It is noteworthy that the MSR operation range is higher than in most of the previous methanol DF engine studies [20,21,25,28] in which MSR normally varies between 0% and 50%. The IMEP of the methanol quantity study was between 4.17 and 13.78 bar.

Fig. 4 shows the cylinder pressure and heat release curves of the methanol quantity study. Fig. 4(a) illustrates the test group when the $FuelMEP_{Diesel}$ = 6.61 bar and Fig. 4(b) depicts the $FuelMEP_{Diesel}$ = 1.49 bar test group. For the $FuelMEP_{Diesel}$ = 6.61 bar cases, DSOI and MSOI are fixed at −10 °CA ATDC, and −6 °CA ATDC, respectively. However, when the $FuelMEP_{Diesel}$ reduced to 1.49 bar, to avoid long-delayed combustion, DSOI and MSOI were advanced to −12 °CA ATDC, and −10 °CA ATDC, respectively. It can be observed that higher MSR leads both to increased and retarded peak pressure due to the gradual increase of the total injected energy.

In the $FuelMEP_{Diesel}$ = 6.61 bar test group (Fig. 4(a)), the $FuelMEP_{Methanol}$ = 5.46, 10.61 and 12.21 bar test points reveal two peaks and a long tail region, while three peaks clearly occur in the points of $FuelMEP_{Methanol}$ = 14.14 and 16.07 bar. The $FuelMEP_{Methanol}$ = 16.07 bar test point is taken as an example in order to analyze the combustion stages. The test point has the first peak between θ_1 and θ_2 (θ_2 < CA5), which is formed from the initial premixed diesel combustion according to the DI diesel conceptual model. After that, diesel diffusion combustion develops in the region $\theta_2$to θ_3 and methanol is also ignited in this region. The combustion in the region of θ_3 to θ_4 of the $FuelMEP_{Methanol}$ = 16.07 bar case has a strong third peak suggesting the development of a methanol diffusion flame. This peak only occurs in the $FuelMEP_{Methanol}$ = 14.14 and 16.07 bar test points because of the high MSR of those two cases, 68.2% and 70.9%, respectively. The last region with low-intensity-combustion is observed between θ_4 and CA90. It is mainly caused by the end combustion of methanol [40]. However, as the diesel combustion is rather early and nearly complete, the combustion region between θ_4 to CA90 is still regarded as a part of the methanol diffusion combustion.

In a similar fashion, the $FuelMEP_{Methanol}$ = 5.46, 10.61, and 12.21 bar cases are also formed by the initial premixed diesel combustion ($\theta_1$to θ_2), diesel pilot diffusion combustion and methanol ignition ($\theta_2$to θ_3). However, the $FuelMEP_{Methanol}$ = 5.46, 10.61, and 12.21 bar cases have a MSR of 45.3%, 61.6% and 65.0%, respectively. At those conditions, the methanol quantity is insufficient to fully develop the main fuel diffusion flame. Hence, the heat release from methanol merges with the diesel diffusion combustion resulting in a long-tail, low-intensity heat release (θ_3 to CA90).

Fig. 4(b) with $FuelMEP_{Diesel}$ = 1.49 bar has a similar trend as Fig. 4(a) while the MSR is operated between 87.6% and 95.3%. Initial premixed diesel combustion forms the HRR between regions θ_1 to θ_2. Then, only one peak occurs on the HRR curve and large amounts of methanol dominate the global heat release. From a heat release point of view, early stage methanol combustion merges with diesel combustion between θ_2 to θ_3. In Fig. 4(b), it is observed that the methanol diffusion combustion is fully developed between θ_3 and θ_4 at the $FuelMEP_{Methanol}$ = 13.15, 15.61, 21.65, and 30.44 bar test points. However, this heat release trend is different to that in Fig. 4(a), where the heat release rate experienced a slight decrease before reaching full methanol diffusion combustion (see $FuelMEP_{Methanol}$ = 14.14, 16.07 bar cases). The reason is that the methanol quantity of the test group in Fig. 4(b) is much larger than that in Fig. 4(a) so methanol diffusing combustion has stronger influence. When the methanol injection duration is too long, it leads to a long tail (θ_4 to CA90) as indicated in the $FuelMEP_{Methanol}$ = 30.44 bar test point. To summarize, the current HPDI of methanol with diesel pilot can be regarded as an overlapping of pilot diesel diffusion combustion and methanol diffusion combustion during which methanol premixed combustion merges with pilot diesel diffusion combustion. Specifically, the HPDI methanol combustion also consists of three stages: the 1st phase of pilot premixed combustion, the 2nd stage of pilot diffusion combustion combined with methanol premixed combustion, and the 3rd phase of methanol diffusion flame development and methanol end combustion.

As shown in Fig. 5, CA5, CA50, and CA90 are delayed when increasing the methanol quantity. As the fuel injection timing is constant, the retard of CA5 is due to the methanol cooling effect which lowers the charge temperature [28,45]. CA50 represents the main combustion and it is also delayed when increase the $FuelMEP_{Methanol}$ since higher methanol quantity retards the main phase of heat release. When we increase the $FuelMEP_{Methanol}$, the main combustion phase switches from diesel ($FuelMEP_{Methanol}$ = 5.46 bar, MSR 45.3%) to methanol ($FuelMEP_{Methanol}$ 16.07 bar, MSR 70.9%) in the $FuelMEP_{Diesel}$ = 6.61 bar test

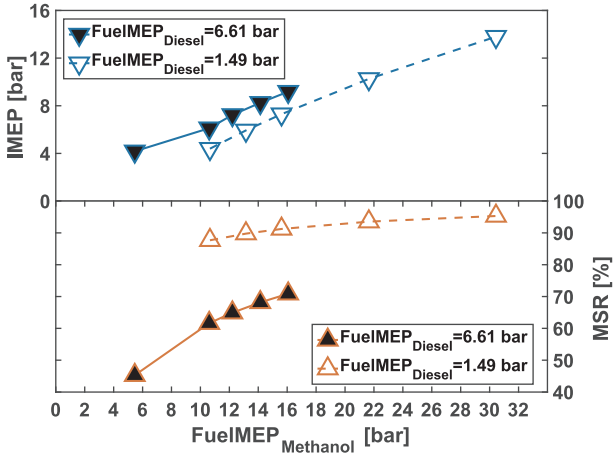

Fig. 3. The Change of IMEP and MSR to the fuel mean effective pressure of Methanol Quantity Study. When $FuelMEP_{Diesel}$ is 6.61 bar, $FuelMEP_{Methanol}$ increases from 5.46 to 16.07 bar, corresponding to 0.95 ms diesel injection duration and 0.65 to 1.15 ms methanol injection duration. When $FuelMEP_{Diesel}$ is 1.49 bar, $FuelMEP_{Methanol}$ rises from 10.66 to 30.44 bar, corresponding to 0.2 ms diesel injection duration and 0.9 to 2 ms methanol injection.

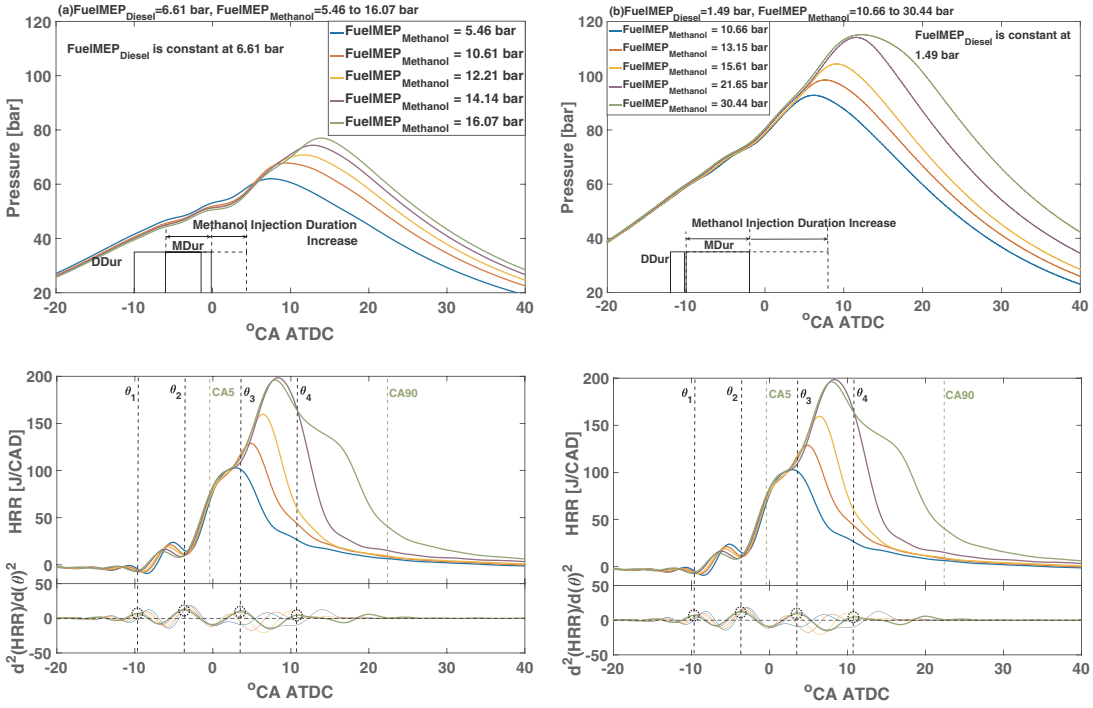

Fig. 4. Cylinder Pressure and HRR Curve of Methanol Quantity Study.

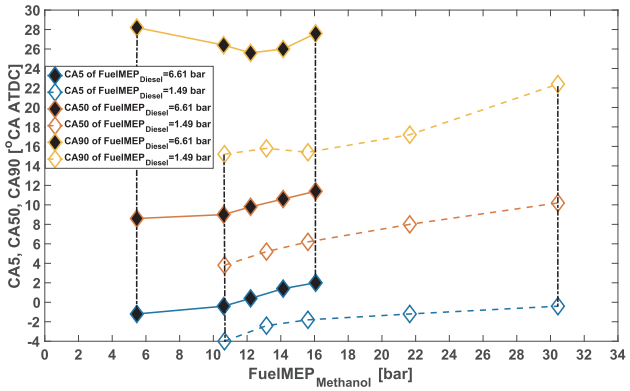

Fig. 5. CA5, CA50, and CA90 of Methanol Quantity Study. FuelMEP$_{Diesel}$ = 6.61 bar, FuelMEP$_{Methanol}$ = 5.46–16.07 bar; FuelMEP$_{Diesel}$ = 1.49 bar, FuelMEP$_{Methanol}$ = 10.66–30.44 bar.

group. While the majority of heat is released from methanol in the FuelMEP$_{Diesel}$ = 1.49 bar test group, the main combustion phase represented by methanol has retarded.

Fig. 6 indicates the changes of combustion duration that is defined as the interval between CA90 and CA5. When we increase the FuelMEP$_{Methanol}$, the combustion duration first decreases and then increases. In the FuelMEP$_{Diesel}$ = 1.49 bar case, the trend from FuelMEP$_{Methanol}$ = 5.46 to FuelMEP$_{Methanol}$ = 14.14 bar is similar to the premixed methanol DF study conducted by Wu and Wei et al. [28,46]. They conclude that higher methanol premixed ratio results in a faster burning rate. Although the current study is non-premixed methanol HPDI mode, DI diffusion flame always starts from premixed combustion at the edge of fuel spray where ∅ is close to one [44]. If the FuelMEP$_{Methanol}$ increases, a larger quantity of injected methanol evaporates due to pilot combustion. The vaporized methanol mixes with air and it results in a higher burning rate in the methanol premixed combustion zone that merges with pilot diffusion combustion. Consequently, combustion duration reduces gradually. However, when methanol injection ends too late, the main combustion phase is excessively retarded (Fig. 4). Subsequently, the turning point of combustion duration occurs at the FuelMEP$_{Methanol}$ = 16.07 bar.

The same trend is observed in the FuelMEP$_{Diesel}$ = 1.49 bar case. More vaporized methanol leads to shorter combustion duration, and retarded end of methanol injection results in increasing combustion duration. When comparing the two curves in Fig. 6, the combustion duration is generally shorter in the FuelMEP$_{Diesel}$ = 1.49 bar test group than that in FuelMEP$_{Diesel}$ = 6.61 bar test group, which is ascribed as the influence of MSR. Methanol contributed to 87.6% to 95.3% of total fuel energy in the FuelMEP$_{Diesel}$ = 1.49 bar test group, while the maximum MSR in the FuelMEP$_{Diesel}$ 6.61 = bar case is 70.8%. In methanol dominant combustion, increased amount of evaporated methanol leads to a higher burning rate in the premixed methanol combustion stage. Hence, the overall combustion duration is shorter in the FuelMEP$_{Diesel}$ = 1.49 bar test group.

Next, we will look at the combustion stability. Fig. 7 shows COV_{IMEP} hat represents the combustion stability of methanol quantity study. In both FuelMEP$_{Diesel}$ = 6.61 bar and FuelMEP$_{Diesel}$ = 1.49 bar test groups, the COV_{IMEP} decreases when increasing methanol quantity. In

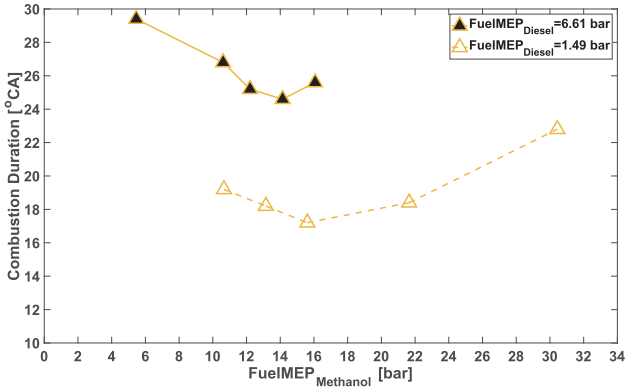

Fig. 6. Combustion Duration of Methanol Quantity Study. FuelMEP$_{Diesel}$ = 6.61 bar, FuelMEP$_{Methanol}$ = 5.46–16.07 bar; FuelMEP$_{Diesel}$ = 1.49 bar, FuelMEP$_{Methanol}$ = 10.66–30.44 bar.

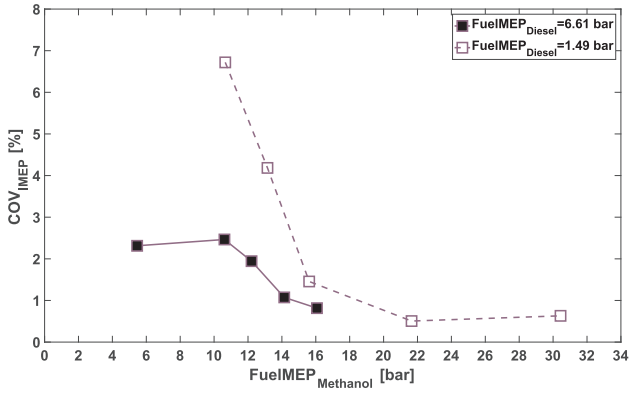

Fig. 7. COV_{IMEP} of Methanol Quantity Study. $FuelMEP_{Diesel}$ = 6.61 bar, $FuelMEP_{Methanol}$ = 5.46–16.07 bar; $FuelMEP_{Diesel}$ = 1.49 bar, $FuelMEP_{Methanol}$ = 10.66–30.44 bar.

the $FuelMEP_{Diesel}$ = 6.61 bar test group, the COV_{IMEP} decreases from 2.2% to 1% $FuelMEP_{Methanol}$ increases from 5.46 bar to 16.07 bar. Similarly, the COV_{IMEP} decreases from 6.8% to 1% in the $FuelMEP_{Diesel}$ = 1.49 bar test group. The behavior of COV_{IMEP} suggests that combustion of high-pressure DI methanol configuration becomes more stable with increased methanol quantity. Both IMEP and MSR changed due to longer main fuel injection duration (Fig. 3), and therefore, the influence of each factor should be examined to clarify the reason for improving the combustion stability. In the present study, COV_{IMEP} is below 1% when IMEP is greater than 8 bar. The reason is that the higher methanol quantity lead to spray guided robust non-premixed combustion. The result suggests that the operation of high MSR is profitable at high IMEP (load) conditions.

Regarding MSR, we find that COV_{IMEP} decreases if MSR increases from 45.3% to 70.9% then further rising to 95.3%. This trend is opposite to the normal methanol PFI dual-fuel engine where COV_{IMEP} rises when MSR is increasing [20]. In PFI methanol engine case, methanol evaporation in the intake port lowers inlet temperature resulting in combustion instability [21]. However, in the present DI methanol study, diesel pilot was always delivered before methanol injection, and subsequently, the strong pilot combustion can offset the negative influence of methanol cooling. When comparing two curves in Fig. 7, MSR indeed has influences on the combustion stability in the HPDI methanol HPDI configuration. At low IMEP conditions, combustion is more stable in the test group of $FuelMEP_{Diesel}$ = 6.61 bar where MSR is 45.3%. However, in the $FuelMEP_{Diesel}$ = 1.49 bar case with the same IMEP condition, MSR is 87.6%. Therefore, the decrease of COV_{IMEP} results mainly from the higher IMEP and diesel pilot combustion. Concerning combustion stability, HPDI of methanol with diesel is advantageous at medium to high IMEP conditions even with high MSR.

Indicated thermal efficiency (ITE) represents the engine performance from a thermodynamic point of view. Fig. 8 illustrates the indicated thermal efficiency of both $FuelMEP_{Diesel}$ = 6.61 bar and $FuelMEP_{Diesel}$ = 1.49 bar test groups. In the $FuelMEP_{Diesel}$ = 6.61 bar case, a higher indicated thermal efficiency is found with more methanol injected as the engine load goes up. In the $FuelMEP_{Diesel}$ = 1.49 bar test group, ITE rises from $FuelMEP_{Methanol}$ = 10.66 bar to 21.65 bar but then drops at $FuelMEP_{Methanol}$ = 30.44 bar test point. Similar to the $FuelMEP_{Diesel}$ = 6.61 bar, efficiency is rising due to higher IMEP. The reason for the decrease of ITE at $FuelMEP_{Methanol}$ = 30.44 bar is due to the significant combustion retarding owing to late end of methanol injection. Additionally, as shown in Fig. 4(b), a long-tail occurs in the HRR curve of $FuelMEP_{Methanol}$ = 30.44 bar, which suggests slow and inefficiency end combustion. As such, the indicated thermal efficiency of $FuelMEP_{Methanol}$ = 30.44 bar is lower than $FuelMEP_{Methanol}$ = 21.65 bar. Overall, it can be seen that HPDI methanol with diesel pilot can achieve relatively high efficiency at high IMEP conditions, and it may be further improved by adjusting the combustion phasing (Section 3.2).

3.1.2. Emission characteristics

Fig. 9(a) illustrates the HC, CO, and NO_x emissions of the methanol quantity study. It is clearly seen that when increasing the $FuelMEP_{Methanol}$, HC emissions decrease dramatically from 23 g/kWh to 2 g/kWh and from 27 g/kWh to 1 g/kWh for both diesel mean effective pressures. The CO emission also shows a decreasing trend. With the $FuelMEP_{Methanol}$ increasing from 5.46 bar to 16.07 bar, CO emission decreases from 4.5 g/kWh to 2.5 g/kWh. Similarly, in Fig. 9(b),

CO continues to drop from 10 g/kWh at $FuelMEP_{Methanol}$ = 10.66 bar to less than 1 g/kWh at $FuelMEP_{Methanol}$ = 30.44 bar. It should be remembered that both MSR and IMEP rise when we increase the methanol fuel quantity; hence, both influences should be considered when analyzing the trend of emissions. we found that although MSR increases, but HC and CO emissions do not increase, which is different from the PFI DF engine study conducted by Chen et al. [47]. This is because DI of methanol with diffusion combustion exhibits less flame extinction or misfire problems (in near-wall regions) compared to premixed combustion [48]. Moreover, with IMEP (load) increasing, HC and CO emissions are reduced significantly because a higher engine load creates more desirable pressure and temperature conditions for methanol combustion. With the increase of IMEP (load), a stronger turbulence and warmer in-cylinder conditions can diminish the unburned methanol problem, which significantly reduce HC emissions.

The tendency of NO_x emission contrasts with that of HC emissions. It increases by 1.5 g/kWh from $FuelMEP_{Methanol}$ = 5.46 bar to $FuelMEP_{Methanol}$ = 16.07 bar in Fig. 9(a), and increments from 2.5 g/kWh at $FuelMEP_{Methanol}$ = 10.66 bar to 5 g/kWh at $FuelMEP_{Methanol}$ = 30.44 bar in Fig. 9(b). This is related to the fact that when the total injected energy is increasing (higher $FuelMEP_{Methanol}$) together with growing ITE, average combustion temperatures are increasing. To summarize, the benefits of operating HPDI methanol configuration at medium and high IMEP are evident concerning emissions, due to the significant reduction of the HC emissions with increasing MSR. Furthermore, only a mild increase in the NO_x emissions is observed when we increase MSR.

3.2. Effects of fuel injection timing

3.2.1. Combustion characteristics

Next, we will study the effect of diesel and methanol injection timings. IMEP is fixed at 6.23 bar and the MSR is constant at 88%. In Fig. 10(a), both the diesel and methanol injection timing (DSOI/MSOI)

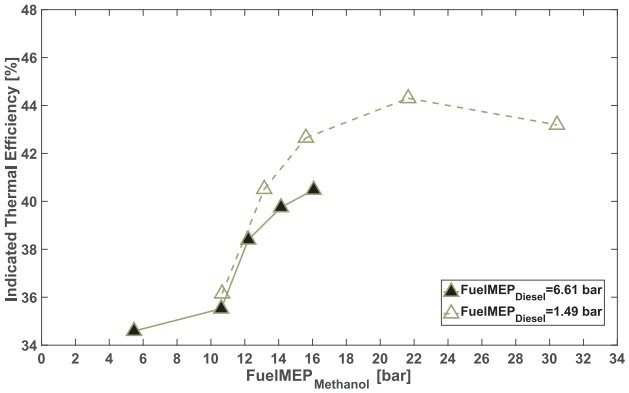

Fig. 8. Indicated Thermal Efficiency of Methanol Quantity Study. $FuelMEP_{Diesel}$ = 6.61 bar, $FuelMEP_{Methanol}$ = 5.46–16.07 bar; $FuelMEP_{Diesel}$ = 1.49 bar, $FuelMEP_{Methanol}$ = 10.66–30.44 bar(a) $FuelMEP_{Diesel}$ = 6.61 bar; $FuelMEP_{Methanol}$ = 5.46–16.07 bar.

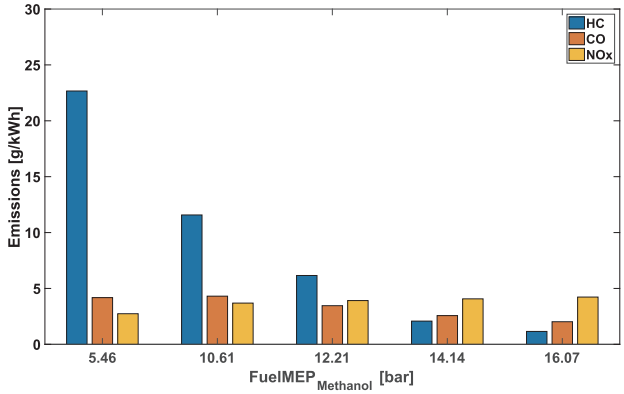

(a)$FuelMEP_{Diesel}$ = 6.61 bar; $FuelMEP_{Methanol}$ = 5.46 to 16.07 bar

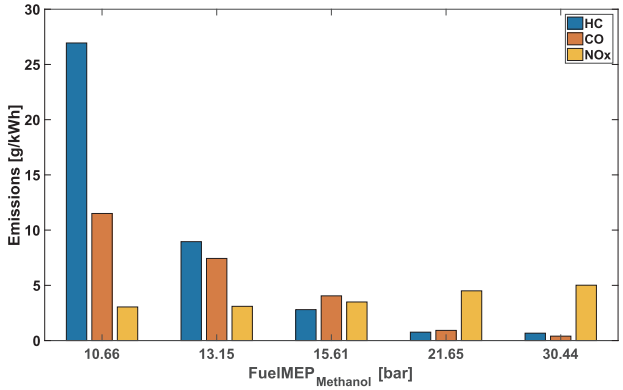

(b)$FuelMEP_{Diesel}$ = 1.49 bar; $FuelMEP_{Methanol}$ = 10.66 to 30.44 bar

Fig. 9. HC, CO, NO_x Emissions of Methanol Quantity Study.

are advanced one crank angle degree per step from −9/−7 °CA ATDC to −13/−11 °CA ATDC as shown in the fuel injection signal. The pressure curve clearly indicates that the combustion is triggered earlier when we advance the DSOI/MSOI timings. Earlier fuel injection also results in higher peak pressure since the combustion starts before TDC as methanol is delivered earlier. Furthermore, the peak pressure is also advanced due to the forward main fuel injection. Regarding the heat release, the HRR curve of each test point merely shifts forward without apparent behavior changes. If we consider DSOI/MSOI at −13/−11 °CA ATDC as an example, the premixed flame forms between θ_1 and θ_2. Diesel pilot diffusion flame and early stage methanol combustion contribute to the combustion between θ_2 and θ_3. The heat release region after θ_3 is due to the main fuel, methanol diffusion combustion. θ_4 refers to the methanol combustion intensity change from high- to low-intensity. The turning θ_3 occurs at all test points, but in contrast to Fig. 4, neither a long tail nor an obvious third peak in the heat release occurs. This is due to methanol being delivered right after the diesel pilot injection, and methanol diffusion combustion being triggered right after pilot combustion. Additionally, the methanol start of injection timing in this test group is earlier than that in Fig. 4, which leaves a longer margin for methanol pre-combustion preparation. Hence, the combustion of methanol is improved and more stable.

Fig. 10(b) illustrates the cylinder pressure and HRR curve of only advancing the diesel injection timing. As the injection signal shown in this test group, DSOI is advanced from −12°CA ATDC to −16 °CA ATDC and MSOI is kept at −10 °CA ATDC. Similar to the advancing DSOI/MSOI set, early pilot injection also leads to the early start of combustion. However, the peak pressure does not rise significantly, because the methanol injection timing and duration are constant in this test group. In addition, the majority of heat release in Fig. 10(b) does not display large changes since methanol accounts for 88% of total energy. The early diesel pilot injection timing only advances the ignition timing, but does not affect the main combustion phasing which is mainly formed by a considerable amount of methanol. The combustion stage is similar to that in and Fig. 10(a). The only difference is that CA5 occurs ahead of θ_2 which is due to early pilot injection. As a result, the majority of heat release in the region between θ_2 to θ_4 comes from methanol. Hence, diesel and methanol diffusion combustion are relatively independent from each other. Fig. 4

Fig. 11 shows that earlier injection of both methanol and diesel advance the combustion. When both DSOI and MSOI are advanced, CA5 is advanced from 0.4 °CA ATDC to −3.2°CA ATDC, and CA50 is advanced from 8.4 °CA ATDC to 4.6 °CA. When only diesel pilot injection

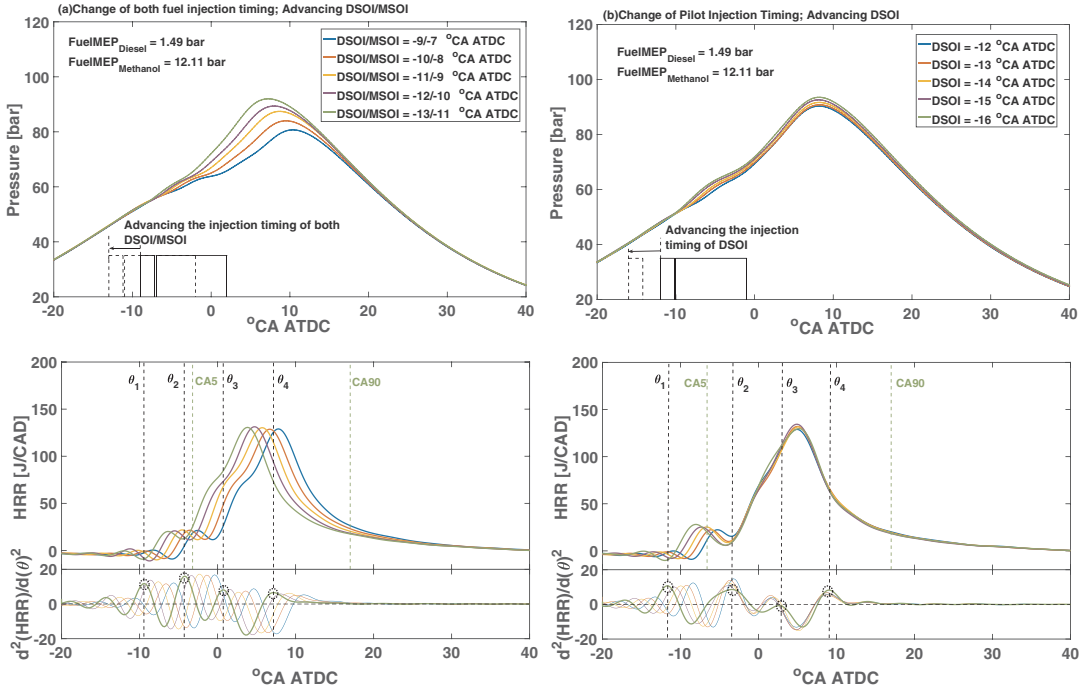

Fig. 10. Cylinder Pressure and HRR Curve of the Fuel Injection Timing Study.

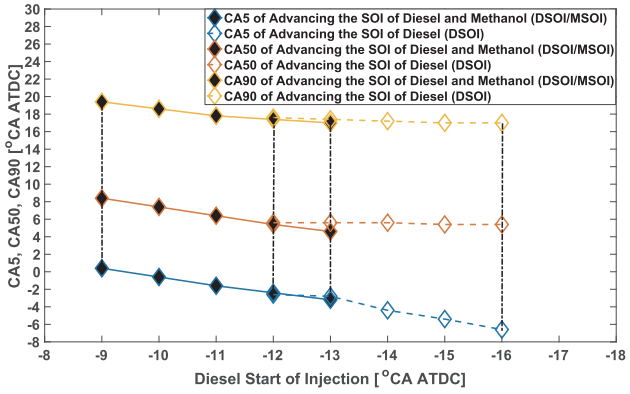

Fig. 11. CA5, CA50, and CA90 of Fuel Injection Timing Study. Advancing both DSOI and MSOI, and only advancing DSOI are tested.

timing was advanced, the combustion phasing remains constant at 5 °CA ATDC. The results suggest that the pilot injection timing directly controls the ignition but the main combustion phase is governed by methanol injection parameters. The ignition stage and the main combustion phasing are less correlated

Besides, the combustion duration can be seen in Fig. 12. The increasing combustion duration when advancing the SOI of both diesel and methanol injection timing is moderate. Hence, the whole combustion event is earlier resulting in only minor changes. However, when advancing the SOI of diesel only, approximately four crank angle degree increase is CA90 is seen. This is reasonable since the start of combustion is earlier while the methanol timing is kept constant.

Fig. 13 indicates the COV_{IMEP} of advancing the fuel injection timing when IMEP was constant at 6.23 bar. It can be seen that advancing the set of DSOI/MSOI or advancing only DSOI can both slightly improve the combustion stability. When advancing both DSOI and MSOI, COV_{IMEP} decreases slightly from 5.6% to 4.9%. This is because an early DSOI/MSOI reserves a longer time for fuel evaporation and atomization, which improves the stability of methanol diffusion flame. When only advancing DSOI, COV_{IMEP} is reduced by 2.5%. This suggests that combustion is more stable if pilot fuel is injected earlier. Similar phenomenon was also observed by Wei et al. [20]. This is because advanced pilot injection and earlier ignition enhance the cylinder conditions for later injected methanol. It is clearly seen from Fig. 13 that combustion is more stable when advancing only DSOI.

When comparing Figs. 13 and 7, the combustion is less stable in the fuel injection timing study. As analyzed in Section 3.1.1 higher IMEP and strong pilot combustion can strengthen the combustion stability. Hence, in this test group, the reason for a less stable combustion is attributed to high MSR and low IMEP. The MSR is constant at 88% so that a large amount of methanol increases the unsteadiness of the combustion. Besides, IMEP is around 6 bar in this test, but IMEP in $FuelMEP_{Methanol}$ = 30.44 bar case is over 13.79 bar. Subsequently, high MSR and low-IMEP yields less stable HPDI methanol combustion.

In the case of advancing the SOI of both diesel and methanol, indicated thermal efficiency increases slightly since CA50 is advanced leading to higher efficiency. On the contrary, indicated thermal efficiency fluctuates with advancing DSOI but does not have an apparent increasing or decreasing trend. This is because the pilot injection timing does not have a strong influence on the methanol combustion phase that governs the combustion. Besides, the amount of diesel is too little to have significant effect on the main combustion phase as illustrated in Fig. 14.

3.2.2. Emission characteristics

Fig. 15(a) and (b) show HC, CO and NO_x emissions when advancing both methanol and diesel injection timing, or advancing only methanol injection timing, respectively. The operation condition is IMEP 6.23 bar and constant 88% MSR. HC emissions reduction can be seen from both Fig. 15(a) and (b), while the changes of CO and NO_x are not obvious. With DSOI/MSOI advancing, less HC emissions are due to the earlier methanol injection providing sufficient time for methanol combustion. The overall HC emissions level in Fig. 15(b) are lower than that in Fig. 15(a). This is because the burning diesel pilot increases the in-cylinder temperature and pressure and, consequently, improves the methanol combustion. The CO emission has no apparent decrease in Fig. 15(a), but it drops by 2 g/kWh in Fig. 15(b), which additionally supports the idea that only advancing DSOI can further benefit the methanol combustion. NO_x emission rises from 2.46 g/kWh to 3.72 g/kWh in Fig. 15(a) and increases from 3.14 g/kWh to 3.83 g/kWh in Fig. 15(b). As discussed in Section 3.1.1, when the SOI gap between DSOI and MSOI is kept at 2°CA, pilot diesel cannot compensate for the cooling effects of a large amount of methanol. On the contrary, when only advancing pilot diesel, the combustion starts earlier (Fig. 10), and the cylinder temperature and pressure are higher during methanol injection. Therefore, NO_x emission is higher to some degree in Fig. 15(b) than in Fig. 15(a). To summarize, advanced fuel injection timing will benefit the methanol HPDI DF combustion with lower HC, CO emissions accompanied by a mild increase of NO_x emission. Specifically, the advanced DSOI creates more beneficial conditions for methanol HPDI DF combustion since it further reduces HC emissions.

4. Discussion

The present study considers the direct injection of methanol ignited by a diesel pilot. Hence, it is principally different to port fuel injection dual-fuel engines, where the combustion is governed by premixed flame propagation. Wei et al. [20] conducted a methanol port injection dual-fuel engine study and observed a significant COV_{IMEP} rise when MSR increased from 10% to 50%. However, in the present study, engine load plays a more important role than the methanol energy ratio. This is also supported by Chen et al. [47] who analyzed COV_{IMEP} of a PFI methanol diesel DF engine at 50%, 75% and 100% loads. They found that combustion was more stable at higher engine load coniditons. Similarly, HC and CO emissions were reduced at higher engine load conditions as observed by Chen and Cheung et al. [47,49].

Regarding the present study, all test points are summarized in an IMEP-MSR diagram (Fig. 16) indicating the promising operation window for HPDI of methanol with diesel pilot. When operating at low IMEP conditions, the combustion is less stable and HC emissions are higher than 20 g/kWh. If IMEP increases, HC emissions decrease gradually. Moreover, test points in blue (Section 3.2) and yellow (3.1) ellipses illustrate the operation conditions around 6–8 bar.

When MSR is about 90%, the HC emissions are high (Fig. 15) and combustion is less stable (Fig. 13), while lower MSR results in lower HC emissions (Fig. 9) and more stable combustion (Fig. 7). Hence, this

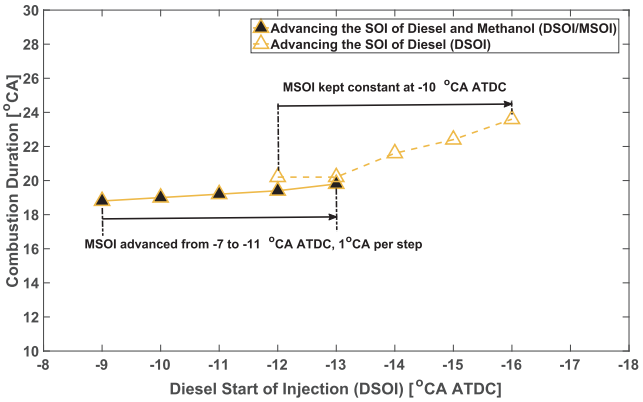

Fig. 12. Combustion Duration of Fuel Injection Timing Study. Advancing both DSOI and MSOI, and only advancing DSOI are tested.

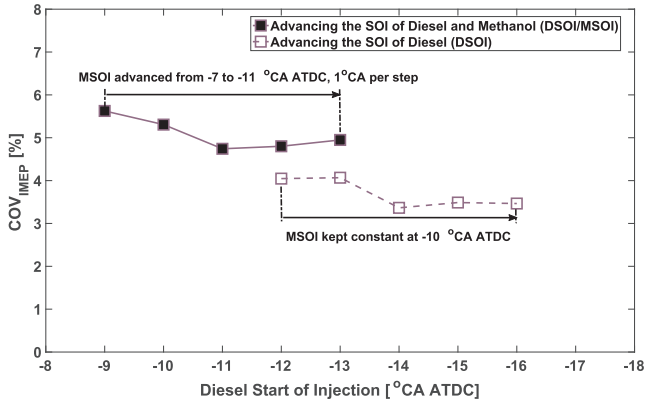

Fig. 13. COV_{IMEP} of Fuel Injection Timing Study. Advancing both DSOI and MSOI, and only advancing DSOI are tested.

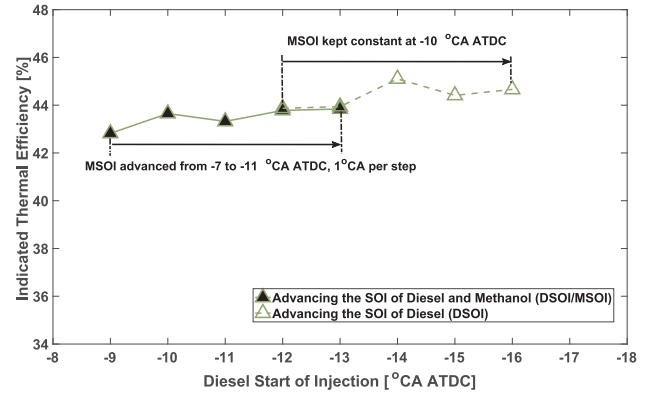

Fig. 14. Indicated Thermal Efficiency of Fuel Injection Timing Study. Advancing both DSOI and MSOI, and only advancing DSOI are tested.

suggests that both MSR and IMEP have impacts to the combustion and emissions. When increasing IMEP above 6 bar, HC emissions decreases dramatically below 1 g/kWh. Based on this observation, a resulting hypothesis is that the promising operation zone for HPDI of methanol is at medium to high IMEP (> 8 bar) and high MSR conditions where the HC emissions are low, combustion is stable and the combustion efficiency of methanol is very high. This is in line with the findings of Ekholm et al. [50] who concluded that medium to high load operation yielded stable combustion, relatively high efficiency, and low emissions in an ethanol-diesel fumigation DF engine.

5. Conclusion

This paper investigated a high-pressure direct injection of methanol with diesel pilot ignition dual-fuel engine. We designed a new cylinder head to accommodate two injectors and conducted experiments at a constant engine speed of 1500 rpm and 16.5 compression ratio. The indicated mean effective pressure (IMEP) varied between 4.2 bar and 13.8 bar while the methanol substitution ratio was kept between 45% and 95%. The influence of methanol quantity and fuel injection timing on the combustion and emission characteristics were investigated. The main results and conclusions are drawn as follows:

1. The combustion of high-pressure direct injection of methanol with diesel pilot has three heat release phases. **Phase I:** diesel pilot ignition and combustion; **Phase II:** diesel diffusion flame development which merges with ignition and early stage methanol combustion; **Phase III:** methanol diffusion flame development which contains a high-intensity and a low-intensity heat release stage. Phase III depends on the methanol injection parameters, namely, methanol injection duration, start of methanol injection and methanol substitution ratio.
2. With low methanol substitution ratio (MSR), methanol diffusion combustion merges with the heat released from pilot diesel combustion.
3. The combustion stability is enhanced at medium to high IMEP conditions even with 94% methanol substitution ratio. Another approach to stabilize the combustion is to advance fuel injection timing. It was found that while keeping the methanol timing constant, advancing the pilot timing was more desirable.
4. The HC emissions are significantly reduced by increasing the IMEP (load) even if the MSR is also increasing. HC emissions can also be reduced by advancing the fuel injection timing. NO_x emissions were

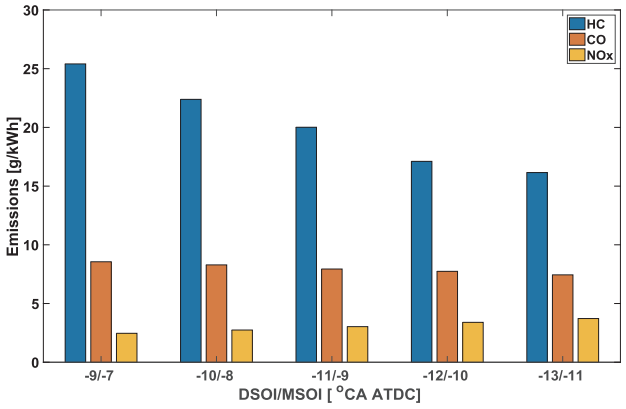

(a)Change of both Fuel Injection Timing; Advancing DSOI/MSOI

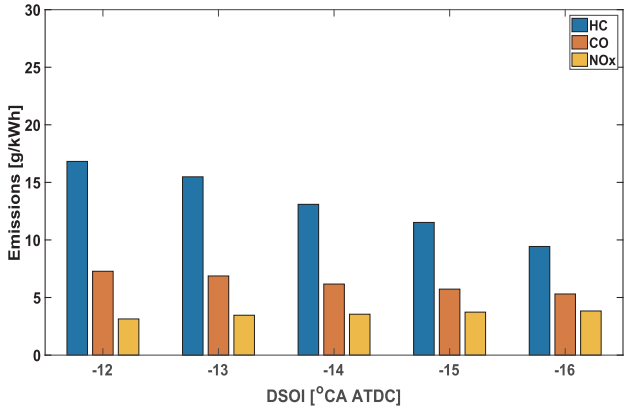

(b)Change of Pilot Injection Timing; Advancing DSOI

Fig. 15. HC, CO and NO_x Emissions of Fuel Injection Timing Study.

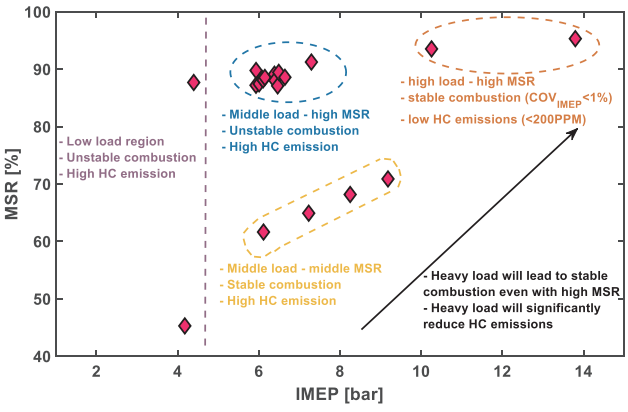

Fig. 16. Summary of Methanol HPDI with Diesel Pilot Dual-Fuel Engine Configuration Operation Points; MSR-IMEP.

low and mildly increasing with increasing IMEP (load).
5. The high-pressure direct injection of methanol with diesel pilot is preferable to be operated above medium engine load conditions (> 8 bar) for stable combustion and low HC emissions.
6. The designed new cylinder head with two injector positions was operating in a robust and consistent manner with no misfire problems.

The present study shows promising performance with more than 90% of methanol substitution ration, low HC emissions, and stable combustion. Especially, we found the present dual-fuel engine configuration was really good with high-load conditions. In a continuation of the present study, the low load points could be improved concerning efficiency and emissions. Future testing to improve these points could be related to the injection pressure of the main fuel as well as to the intake air temperature.

CRediT authorship contribution statement

Yabin Dong: Methodology, Formal analysis, Writing - review & editing. **Ossi Kaario:** Conceptualization, Formal analysis, Writing - review & editing. **Ghulam Hassan:** . **Olli Ranta:** . **Martti Larmi:** Supervision, Funding acquisition. **Bengt Johansson:** Conceptualization.

Declaration of Competing Interest

The authors declare that they have no known competing financial interests or personal relationships that could have appeared to influence the work reported in this paper.

References

[1] World Energy Balances 2018. International Energy Agency, Paris; 2018.
[2] Pedrozo VB, May I, Macklini Dalla Nora AC, Zhao H. Experimental analysis of ethanol dual-fuel combustion in a heavy-duty diesel engine: an optimisation at low load. Appl Energy 2016;165:166–82.
[3] Wallington T, Lambert C, Ruona W. Diesel vehicles and sustainable mobility in the U.S. Energy Policy 2013;54:47–53.
[4] International Energy Outlook 2016. U.S. Energy Information Administration, Washington; 2016.
[5] Jr RFB, Martins CA. Experimental analysis of a diesel engine operating in diesel-ethanol dual-fuel mode. Fuel 2014;134:140–50.
[6] Yao M, Zheng Z, Liu H. Progress and recent trends in homogeneous charge compression. Prog Energy Combust Sci 2009;35:398–437.
[7] Kook S, Bae C. Combustion control using two-stage diesel fuel injection in a single-cylinder PCCI engine. SAE Technical Papers 2004–01-0938,:2004.
[8] Reitz RD, Duraisamy G. Review of high efficiency and clean reactivity controlled compression. Prog Energy Combust Sci 2015;46:12–71.
[9] Rahman KA, Ramesh A. Studies on the effects of methane fraction and injection strategies in a biogas diesel common rail dual fuel engine. Fuel 2019;236:147–65.
[10] Liu J, Yang F, Wang H, Ouyang M, Hao S. Effects of pilot fuel quantity on the emissions characteristics of a CNG/diesel dual fuel engine with optimized pilot injection timing. Appl Energy 2013;110:201–6.
[11] Schlatter S, Schneider B, Wright YM, Boulouchos K. N-heptane micro pilot assisted methane combustion in a Rapid Compression Expansion Machine. Fuel 2016;179:339–52.
[12] Dong S, Wang Z, Yang C, Ou B, Lu H, Xu H, et al. Investigations on the effects of fuel stratification on auto-ignition and combustion process of an ethanol/diesel dual-fuel engine. Appl Energy 2018;230:19–30.
[13] Boretti A. Advantages of converting diesel engines to run as dual fuel ethanol-diesel. Appl Therm Eng 2012;47:1–9.
[14] Sarjovaara T, Alantie J, Larmi M. Ethanol dual-fuel combustion concept on heavy duty engine. Energy 2013;63:76–85.
[15] Sahoo B, Sahoo N, Saha U. Effect of engine parameters and type of gaseous fuel on the performance of dual-fuel gas diesel engines—a critical review. Renew Sustain Energy Rev 2009;13:1151–84.
[16] Blasio GD, Belgiorno G, Beatrice C. Effects on performances, emissions and particle size distributions of a dual fuel (methane-diesel) light-duty engine varying the compression ratio. Appl Energy 2017;204:726–40.
[17] Papagiannakis R, Rakopoulos C, Hountalas D, Rakopoulos D. Emission characteristics of high speed, dual fuel, compression ignition engine operating in a wide range of natural gas/diesel fuel proportions. Fuel 2010;89:1397–406.
[18] Lounci M, Loubar K, Tarabet L, Balistrou M, Niculescu D, Tazerout M. Towards improvement of natural gas-diesel dual fuel mode: an experimental investigation on performance and exhaust emissions. Energy 2014;64:200–11.
[19] Li G, Zhang C, Li Y. Effects of diesel injection parameters on the rapid combustion and emissions of an HD common-rail diesel engine fueled with diesel-methanol dual-fuel. Appl Therm Eng 2016;108:1214–25.
[20] Wei H, Yao C, Pan W, Han G, Dou Z, Wu T, et al. Experimental investigations of the effects of pilot injection on combustion and gaseous emission characteristics of diesel/methanol dual fuel engine. Fuel 2017;188:427–41.
[21] Liu J, Yao A, Yao C. Effects of diesel injection pressure on the performance and emissions of a HD common-rail diesel engine fueled with diesel/methanol dual fuel. Fuel 2015;140:192–200.
[22] Bertau M, Offermanns H, Plass L, Schmidt F, Wernicke H-J. Methanol: The Basic Chemical and Energy Feedstock of the Future. Springer; 2014.
[23] Bozzano G, Manenti F. Efficient methanol synthesis: perspectives, technologies and optimization strategies. Prog Energy Combust Sci 2016;56:71–105.
[24] Blanco H, Nijs W, Ruf J, Faaij A. Potential for hydrogen and power-to-liquid in a low-carbon EU energy system using cost optimization. Appl Energy 2018;232:617–39.
[25] Pan W, Yao C, Han G, Wei H, Wang Q. The impact of intake air temperature on performance and exhaust emissions of a diesel methanol dual fuel engine. Fuel 2015;162:101–10.
[26] Shamun S, Hasimoglu C, Murcak A, Andersson O, Tuner M. Experimental investigation of methanol compression ignition in a high compression ratio HD engine using a Box-Behnken design. Fuel 2017;209:624–33.
[27] Geng P, Yao C, Wei L, Liu J, Wang Q, Pan W, et al. Reduction of PM emissions from a heavy-duty diesel engine with diesel/methanol dual fuel. Fuel 2014;123:1–11.
[28] Wu T, Yao A, Yao C, Pan W, Wei H, Chen C, et al. Effect of diesel late-injection on combustion and emissions characteristics of diesel/methanol dual fuel engine. Fuel 2018;233:317–27.
[29] Yang B, Xi C, Wei X, Zeng K, Lai M-C. Parametric investigation of natural gas port injection and diesel pilot injection on the combustion and emissions of a turbo-charged common rail dual-fuel engine at low load. Appl Energy 2015;143:130–7.
[30] Ryu K. Effects of pilot injection timing on the combustion and emissions characteristics in a diesel engine using biodiesel–CNG dual fuel. Appl Energy 2013;111:721–30.
[31] Yousefi A, Birouk M. Investigation of natural gas energy fraction and injection timing on the performance and emissions of a dual-fuel engine with pre-combustion chamber under low engine load. Appl Energy 2017;189:492–505.
[32] Papagiannakis R, Hountalas D, Rakopoulos C. Theoretical study of the effects of pilot fuel quantity and its injection timing on the performance and emissions of a dual fuel diesel engine. Energy Convers Manage 2007;48:2951–61.
[33] Ahmad Z, Aryal J, Ranta O, Kaario O, Vuorinen V, Larmi M. An Optical Characterization of Dual-Fuel. SAE Technical Paper 2018-01-0252; 2018.
[34] Wagemakers A, Leermakers C. Review on the effects of dual-fuel operation, using diesel and gaseous fuels, on emissions and performance. SEA Technical Paper 2012-01-0869; 2012.
[35] Abd-Alla G, Soliman H, Badr O, Abd-Rabbo M. Effects of diluent admissions and intake air temperature in exhaust gas recirculation on the emissions of an indirect injection dual fuel engine. Energy Convers Manage 2001;42:1033–45.
[36] Wang Y, Wang H, Meng X, Tian J, Wang Y, Long W, et al. Combustion characteristics of high pressure direct-injected methanol ignited T by diesel in a constant volume combustion chamber. Fuel 2019;254.
[37] Jia Z, Denbratt I. Experimental investigation into the combustion characteristics of a methanol-Diesel heavy duty engine operated in RCCI mode. Fuel 2018;226:745–53.
[38] Faghani E, Kheirkhah P, Mabson C, McTaggart-Cowan G, Kirchen P, Rogak S. Effect of injection strategies on emissions from a pilot-ignited direct-injection natural-gas engine-Part I: late post injection. SAE Technical Paper 2017-01-0774; 2017.
[39] Faghani E, Kheirkhah P, Mabson C, McTaggart-Cowan G, Kirchen P, Rogak S. Effect of injection strategies on emissions from a pilot-ignited direct-injection natural-gas engine-Part II: slightly premixed combustion. SAE Technical Paper 2017-01-0763; 2017.
[40] Ahmad Z, Kaario O, Qiang C, Vuorinen V, Larmi M. A parametric investigation of diesel/methane dual-fuel combustion progression/stages in a heavy-duty optical engine. Appl Energy 2019;251.
[41] Olsson J-O, Tunestål P, Ulfvik J, Johansson B. The effect of cooled EGR on emissions and performance of a turbocharged HCCI engine. SAE Technical Paper, 2003-01-0743; 2003.
[42] Karlm G. Combustion in gas fueled compression: ignition engines of the dual fuel type. J Eng Gas Turbines Power July 2003;125:827–36.
[43] Pettinen R, Kaario O, Larmi M. Dual-Fuel Combustion Characterization on Lean Conditions and High Loads. SAE Technical Paper 2017-010759; 2017.
[44] Dec JE. A conceptual model of DI diesel combustion based on laser-sheet imaging. SAE Technical Paper 970873; 1997.
[45] Wei L, Yao C, Han G, Pan W. Effects of methanol to diesel ratio and diesel injection timing on combustion, performance and emissions of a methanol port premixed diesel engine. Energy 2016;95:223–32.
[46] Wei L, Yao C, Quangang W, Pan W, Han G. Combustion and emission characteristics of a turbocharged diesel engine. Fuel 2015;140:156–63.
[47] Chen Z, Yao C, Yao A, Dou Z, Wang B, Wei H, et al. The impact of methanol injecting position on cylinder-to-cylinder variation in a diesel methanol dual fuel engine. Fuel 2017;191:150–63.
[48] Li Y, Jia M, Chang Y, Liu Y, Xie M, Wang T, et al. Parametric study and optimization of a RCCI (reactivity controlled compression ignition) engine fueled with methanol and diesel. Energy 2014;65:319–32.
[49] Cheung C, Zhang Z, Yao TCAC. Investigation on the effect of port-injected methanol on the performance and emissions of a diesel engine at different engine speeds. Energy Fuels 2009;23:5684–94.
[50] Ekholm K, Karlsson M, Tunestål P, Johansson RJAB. Ethanol-Diesel Fumigation in a Multi-Cylinder Engine. SAE Technical Paper, 2008-01-0033; 2008.